Microchim Acta (2013) 180:303–310
DOI 10.1007/s00604-012-0934-y

ORIGINAL PAPER

Sensitive immunoassay for porcine pseudorabies antibody based on fluorescence signal amplification induced by cation exchange in CdSe nanocrystals

XuePu Li · Kun Chen · Liang Huang · DongLian Lu · JianGong Liang · HeYou Han

Received: 4 September 2012 / Accepted: 10 December 2012 / Published online: 28 December 2012

Abstract We report on a novel immunoassay for porcine pseudorabies virus (PRV) antibody that is based on fluorescence signal amplification induced by silver(I) ion exchange in CdSe nanocrystals. An antigen-antibody-secondary antibody sandwich structure was first formed from PRV, PRV antibody, and CdSe-labeled rabbit anti-pig antibody. Then, the Cd(II) ions in the CdSe labels were released by a cation exchange reaction with Ag(I). Released Cd(II) was finally quantified using the sensitive fluorescent probe Rhodamine 5 N. Due to this signal amplification, the sensitivity and linear range of the immunoassay were largely improved (compared to the traditional ELISA) in having a limit of detection as low as 1.2 ngmL^{-1} of PRV antibody and a linear range from 2.44 to 312 ngmL^{-1}. The successful determination of PRV antibody in pig serum samples is proof for the utility of the method.

Keywords Porcine pseudorabies virus · Immunoassay · Fluorescence signal amplification · Cation-exchange · CdSe nanocrystals

Introduction

Porcine pseudorabies is an acute, frequently fatal epidemic disease which infects not only pigs but other animals such as cattle, cats and sheep and so on [1]. The main pathogen caused the porcine pseudorabies is porcine pseudorabies virus (PRV), which belongs to the Herpesviridae, *Suid herpesvirus 1* [2]. Animal infected porcine pseudorabies usually has some apparent symptoms; the most prominent involves the nervous and respiratory systems [3, 4]. In Asia and Europe, porcine pseudorabies has been regarded as an important cause of death in pigs of all ages and as a cause of abortion in sow [5].

Until now, there is no effective therapy for the infected pigs; it causes enormous economic losses to animal husbandry worldwide. To block the frightening spread of porcine pseudorabies, early diagnosis and isolation of the infected pigs are very important [6–8]. Now, most common methods used to detect animal diseases still focus on some traditional means, including the virus neutralization [9], enzyme linked immunosorbent assay (ELISA) [10] and Polymerase Chain Reaction [11, 12]. Among them, ELISA is the most frequently used method for the detection of porcine pseudorabies. In the immunoassay such as ELISA, different enzymes including alkaline phosphatase [13–15], horseradish peroxidase [16–18] and glucose oxidase [19] are commonly used as labels for signal amplification and to produce a detectable signal for the detection. However, the colorimetry has a relative low sensitivity, thus the detection limit and linear range are very limited [20, 21]. Therefore, developing sensitive and quantitative detection methods for porcine pseudorabies is quite necessary.

Compared with enzymes, nanomaterial as signal amplification labels have many particular advantages such as low cost, good stability under extreme conditions and the signals can be detected by numerous ways. Fluorescence [22], absorption spectrum [19], surface enhanced Raman scattering (SERS) [23] and electrochemical analysis [24, 25] all have been successfully used in the immunoassay for signal amplification based on the nanomaterial. Recently, cation-exchange in nanocrystals to release metal ions provides a

Electronic supplementary material The online version of this article (doi:10.1007/s00604-012-0934-y) contains supplementary material, which is available to authorized users.

X. Li · K. Chen · L. Huang · D. Lu · J. Liang · H. Han (✉)
State Key Laboratory of Agricultural Microbiology,
College of Science, Huazhong Agricultural University,
Wuhan 430070, People's Republic of China
e-mail: hyhan@mail.hzau.edu.cn

novel signal amplification method for immunoassay owing to the thousands of metal ions contained in nanocrystals [26, 27]. Kucur et al. reported that there are 2,051 Cd^{2+} in a CdSe nanocrystals with a diameter 5.15 nm and 2,200 more Cd^{2+} were enclosed with the increment 1 nm [28]. Moreover, such approaches are also very simple, low-cost, and have no strict requirements on the optical, shapes or other properties of the nanocrystals. The released metal ions also can be detected by many ways such as fluorescence indicator quenching or enhancement, chemiluminescence enhancement and electrochemical analysis [27, 29–31].

Herein, we report a simple, rapid and sensitive method for the detection of PRV antibody through the caused by cation-exchange in CdSe nanocrystals. The principle was shown in scheme 1. The CdSe nanocrystals labeled rabbit anti-pig IgG was used to capture the PRV antibody. After the immunoreaction, the Cd^{2+} in the CdSe labels was completely replaced by the cation-exchange reaction with Ag^{+}. Then Cd^{2+}sensitive fluorescence indicator Rhodamine 5 N was added to bind with Cd^{2+} and caused the fluorescence signal enhance substantially. Thus a novel method for rapid and sensitive detection of porcine pseudorabies was developed. Further, the method has been successfully applied in detection PRV antibody directly in clinical serum samples.

Experimental

Reagents

The polystyrene 96 well plates obtained from Wuhan keqian Animal Biological Products Co. Ltd. of China (http://www.kqbio.com/) were used to perform the immunoreactions. Rhodamine 5 N was purchased from Invitrogen Corporation of California (http://www.invitrogen.com/) and dissolved in ultrapure water, stored at −20 °C.1-ethyl-3-(3-(dimethylamino) propyl) carbodiimide hydrochloride (EDC) and N-hydroxysuccinimide (NHS), Trioctylphosphine oxide (TOPO, 90 %), hexadecylamine (HDA, 90 %), stearic acid (SA, 95 %), cadmium oxide (CdO, 99.99 %), selenium powder (99.99 %), mercaptopropionic acid (MPA, 99 %) and dioctylamine (DOA, 90 %) were obtained from Sigma Aldrich company of America (http://www.sigmaaldrich.com/china-mainland.html). The rabbit anti-pig IgG and HRP labeled rabbit anti-pig IgG were purchased from Biosynthesis Biotechnology Co. Ltd of China (http://www.bioss.com.cn/). The PRV, PRV antibody, positive and negative serum of PRV and Porcine Reproductive and Respiratory syndrome virus (PRRSV) were also obtained from Wuhan keqian Animal Biological Products Co. Ltd (http://www.kqbio.com/). All other reagents used in the experiment were analytical grade and used without further purification. Ultrapure water (18.25 MΩ cm) was used throughout the experiments.

Apparatus

Perkin Elmer 1420 Multilabel Counter (http://www.perkinelmer.com/) was used for fluorescence and optical density (OD) measurement. The hydrodynamic size was measured by dynamic light scattering on Malvern Zetasizer Nanoseries (http://www.malvern.com/labeng/products/zetasizer/zetasizer.htm) using 633 nm laser at 25 °C. Ultraviolet–visible (UV–vis) absorption spectra were recorded on Nicolet Evolution 300 Ultraviolet–visible spectrometer (Thermo Nicolet, US. http://www.thermoscientific.com). Photoluminescence (PL) spectra were measured on Edinburgh FLS920 spectrometer (λ_{ex}=535 nm, λ_{em}=575 nm) equipped with a quartz cell (1 cm×1 cm) (http://www.edinburghphotonics.com/spectrometers/). Transmission electron microscope (TEM) images were obtained by using a Tecnai G20 microscope (FEI, Czech Republic, http://cme.espe.edu.ec/en/).

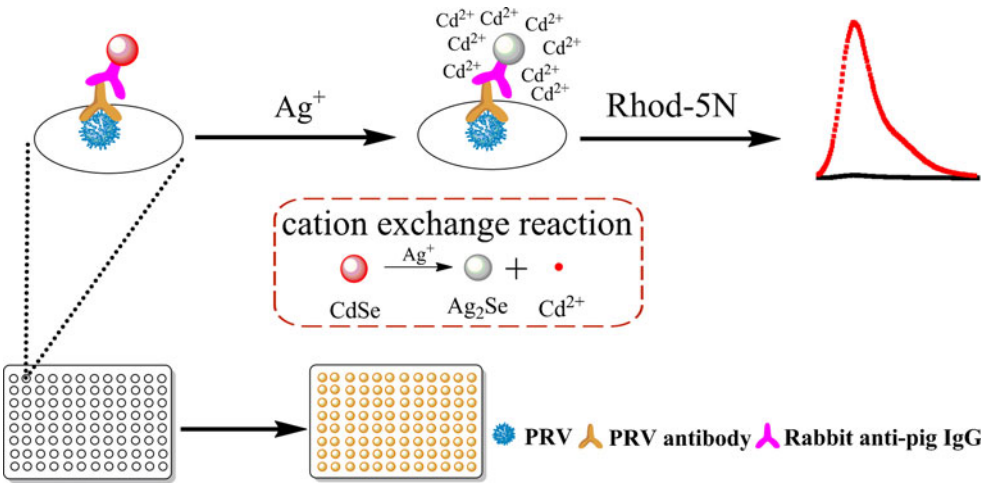

Scheme 1 The principle of the method for detection of PRV antibody

Synthesis water-soluble CdSe nanocrystals

The CdSe nanocrystals were prepared according to the method described previously with slight modifications [32]. In the synthesis, 1.96 g TOPO, 1.96 g HDA and cadmium precursor Cd (SA) $_2$ (prepared by heating 0.1 mmol CdO and 0.4 mmol SA under N_2 flow at 150 °C until the solution become clear) were mixed in a dried 3 necked-flask and heated to 260 °C under N_2 flow. A selenium solution containing 1 mmol selenium powder, 1 mL TOP and 2 mL DOA was injected into the flask quickly. After 1 min, the mixture turned to be wine and the reaction was stopped. Cooled it to room temperature, then 35 mL methanol and 15 mL chloroform were added to the mixture to precipitate the nanocrystals. The nanocrystals were further purified by centrifuged at 12,000 rpm three times. The sediments obtained were dissolved in 5 ml chloroform for following use.

The TOPO and HDA coated CdSe nanocrystals were transferred from chloroform to the aqueous phase by replace the TOPO and HDA with MPA [33]. In a typical phase transfer procedure, the same volume ultrapure water contained 5,000 fold MPA was mixed with the CdSe nanocrystals solution, and then adjusted the pH to 8.0 by using saturated NaOH solution. After stirring about 5 h, the CdSe nanocrystals were transferred to the aqueous phase. Then the aqueous solution was ultra-filtrated three times by using a 30 KD Millipore ultrafiltration tube to remove the excess MPA.

Bioconjugation of CdSe nanocrystals with antibodies

EDC and NHS were used as coupling reagents to couple the CdSe nanocrystals with rabbit anti-pig IgG. 100 μL CdSe nanocrystals was mixed with 50 μL EDC (0.05 mol) and 30 μL NHS (0.1 mol) for 30 min to activate the carboxyl of the MPA, then 200 μL rabbit anti-pig IgG were added to the solution and stirred for 2 h at the room temperature. To avoid the protein crossing coupling, 1.0 μL 2-mercaptoethanol was used to quench the residual EDC after the activation. Finally, to remove the excess IgG, the mixture was ultra-filtrated three times by using a 100 KD Millipore ultrafiltration tube. The antibody after conjugate was diluted 100 fold and stored at 4 °C for the following experiments.

Procedure for the PRV antibody detection

The immunoassay was performed on the polystyrene 96-well plates. Firstly, the 96 well plates were coated with PRV by overnight at 4 °C, and then the wells were blocked with 1 % BSA for 30 min at 36 °C. After blocking, 100 μL PRV antibody solutions with different concentration were added to the wells and incubated for 1 h at 36 °C. After the incubation, the wells were washed with phosphate buffer (0.01 M phosphate and 0.05 % Tween-20) for 3 times and 5 min each time. Secondly, 100 μL CdSe nanocrystals labeled rabbit anti-pig IgG was added to the wells. The plates were incubated for 1 h at 36 °C and washed as the previous procedure. Finally, 200 μL 0.1 M KAc-0.05%Tween 20 buffer contained 3.0 μM Rhodamine 5 N and 200 μM Ag^+ was added for the fluorescence measurement.

Result and discussion

Characterization of CdSe nanocrystals and CdSe nanocrystals-antibody conjugate

The UV—vis absorption spectrum and fluorescence spectrum were employed to characterize the CdSe nanocrystals. As shown in Fig. 1A, compared with the strong fluorescence signal before phase transfer, the fluorescence intensity of the CdSe nanocrystals in water had been quenched by thiolated ligands (MPA). The excess thiolated ligands are favorable to the stability of the nanocrystals but usually results a quenching of the fluorescence [34]. The transmission electron microscope of CdSe nanocrystals before and after phase transfer were shown in Fig. 1B, it can be seen that the average size is about 4.5 nm in diameter and the shapes of CdSe nanocrystals are spherical, monodisperse. The homogeneous distribution in aqueous solution also demonstrated the good stability of the nanocrystals after phase transfer.

After the conjugation, the average hydrodynamic size of CdSe increased from 5.96 nm to 29.8 nm as illustrated in Fig. 1C. The average hydrodynamic size of rabbit anti-pig was 9.60 nm (Fig. 1C) and the theoretical value of the conjugates was 25.2 nm (5.96 nm +9.60 nm +9.60 nm=25.16 nm). In the measurement, different IgG-to-nanocrystals molar rations and different spatial conformations are all possible, the additional solvent molecules layer are also migrate together with the nanoparticle, so the measured average hydrodynamic size usually are not entirely consistent with the theoretical value [35]. Compared with the theoretical value 25.16 nm, the measured results 29.8 nm are acceptable and indicated that the rabbit anti-pig was successfully conjugated with the CdSe nanocrystals.

Optimizing the signal generated by Cd^{2+}

Rhodamine 5 N as a fluorescent dye has very low fluorescence signal due to the intramolecular photoinduced electron transfer. By bound with Cd^{2+}, the photoinduced electron transfer process is reduced which lead to a great enhancement of the fluorescence intensity, therefore Rhodamine 5 N usually act as a fluorescence indicator of the Cd^{2+} [36]. The high level of Rhodamine 5 N usually provides a strong signal; however, the

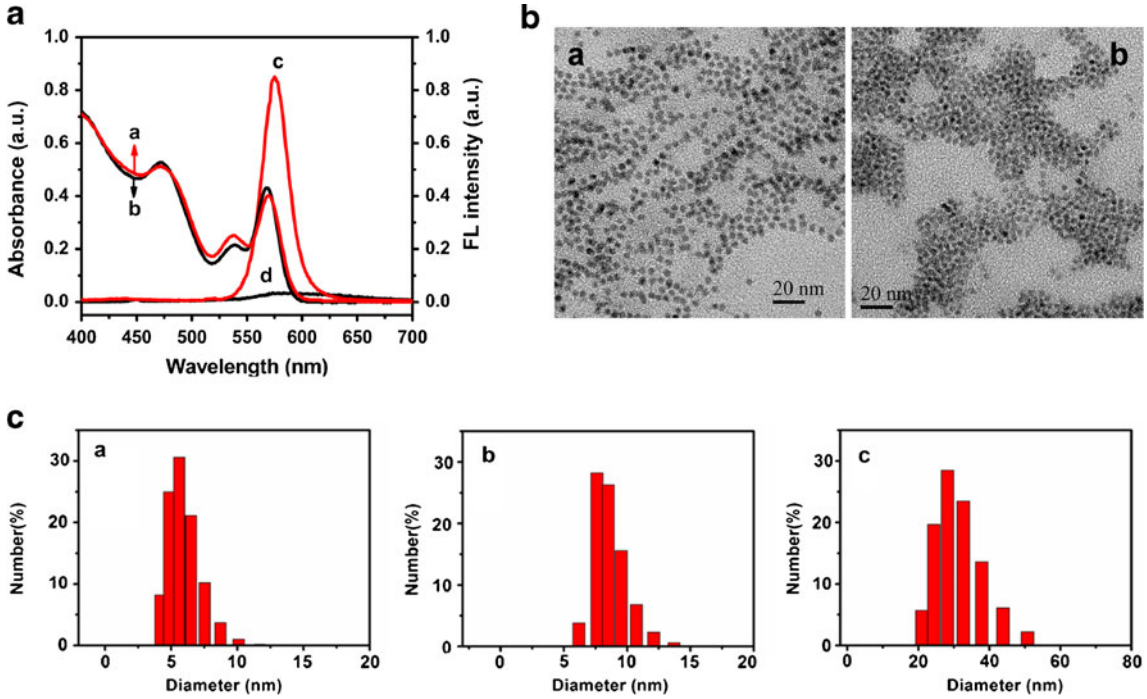

Fig. 1 (**A**) The normalized UV–vis absorption and fluorescence spectra of CdSe nanocrystals (**a**) (**c**) before and (**b**) (**d**) after phase transfer, (**B**) TEM image of CdSe nanocrystals (**a**) before and (**b**) after phase transfer, (**C**) the average hydrodynamic size of (**a**) CdSe nanocrystals (**b**) rabbit anti-pig IgG (**c**) conjugates of the CdSe nanocrystals and rabbit anti-pig IgG

background signal is also strong. To obtain a maximum signal/background ratio, the responses of different concentration Rhodamine 5 N to Cd^{2+} were investigated. As showed in Fig. 2A, the ratios increased very slowly when the concentration was above 2 μM and tend to be saturated when the concentration attained 3 μM. In view of the little difference between the ratio of 3.0 μM and 5.0 μM, 3.0 μM Rhodamine 5 N was adopted in the following experiments.

Cation exchange as a common phenomenon has been widely investigated in many different nanocrystals. Son have reported that Ag^+ can replace the Cd^{2+} in the CdSe nanocrystals to produce Ag_2Se and Cd^{2+}, the reaction occurs completely and fully reversible at room temperature [37]. Herein, we investigated the effect of different level of Ag^+ in the cation exchange. The results showed that at the low concentration of CdSe (0–0.5 nM), the fluorescence signal didn't show a very sensible difference while at the range 0.5 to 5.0 nM, the fluorescence signal gradually increased with the increment of the Ag^+ (Fig. 2B). Cation exchange is a reversible reaction, excess Ag^+ caused the exchange reaction more completely, thus the fluorescence signal had a slightly increment. However, the changes of fluorescence signal was not very obvious when the Ag^+ arrived 200 μM and in the following experiment, the level of CdSe would not reach the saturated concentration, so 200 μM Ag^+ was competent in the detection.

Detection of CdSe nanocrystals using rhodamine 5 N

Though the CdSe NCs have been ultra-filtrated after phase transfer, there are still little residual Cd^{2+} in the solution. The water-soluble CdSe nanocrystals also emitted fluorescence at 575 nm when excited at 390 nm. To investigate the potential effect in the detection, the fluorescence intensity of CdSe nanocrystals and Rhodamine 5 N under different conditions were measured. Figure 3 showed the fluorescence spectrum of the CdSe, Rhodamine 5 N and the response of the Rhodamine 5 N to CdSe nanocrystals, Ag^+, and mixture of CdSe nanocrystals with Ag^+ respectively. Compared with the fluorescence signal after cations exchange, the background signal (Rhodamine 5 N) and the fluorescence signal of the CdSe were both very low. The obtained fluorescence signals before and after cations exchange showed a 58 fold enhancement and the signal after cations exchange are 370 fold of the water-soluble CdSe NCs. The low fluorescent signal of the Rhodamine 5 N with Ag^+ indicated that Ag^+ didn't interfere the assay and was suitable for our experiment. Compared with the signal of Rhodamine 5 N, the slightly increment after adding the CdSe suggested that there were still little residual Cd^{2+} in the CdSe solution. The main reason may be that: 1) the low LOD (3 nM) of Cd^{2+} using the Rhodamine 5 N as an indicator [36] 2) the solubility equilibrium of CdSe in the solution also can't be neglected due to the large surface-area-to-volume ratio of CdSe Nanocrystals [37]. However, the signal after

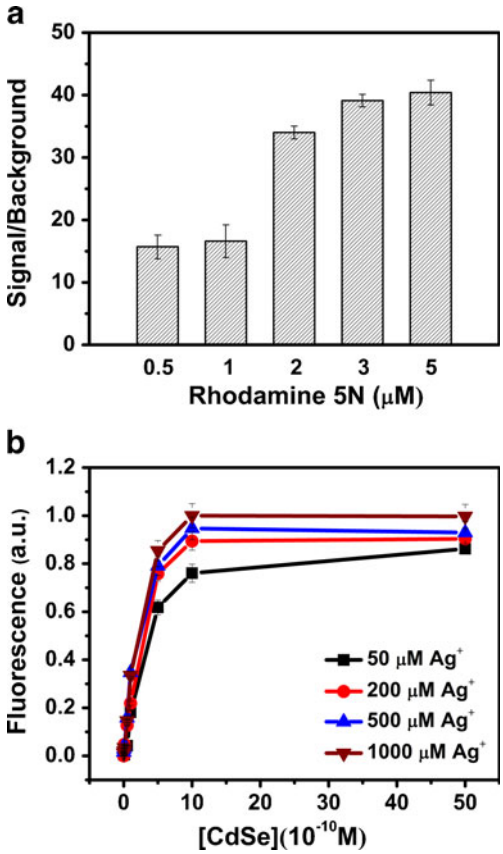

Fig. 2 (**A**) Comparison of different signal $_{(cd^{2+}=5\ \mu M)}$/background $_{(cd^{2+}=0\ \mu M)}$ ratio with 0.5, 1.0, 2.0, 3.0 and 5.0 μM Rhodamine 5 N in 0.1 M KAc-0.05%Tween 20 buffer. The Cd^{2+} used in the experiment was 1.0 μM. (**B**) Detection Cd^{2+} with 50, 200, 500 and 1,000 μM Ag^{+} in 0.1 M KAc-0.05%Tween 20 buffer. The signals were all normalized. Each point depicted the average measurements of three times. Error bars were calculated based on the standard deviation of three measurements

cation-exchange was so intensive, the slightly increment had no interference on the detection.

In the immunoassay, the CdSe labeled antibody was firstly captured by the PRV antibody, and then the Cd^{2+} contained in the CdSe was replaced by Ag^{+} immediately.

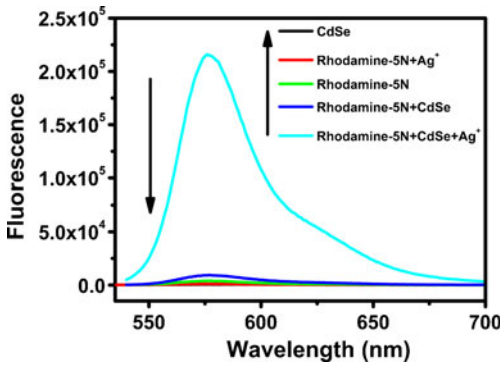

Fig. 3 Fluorescence spectrum of Rhodamine 5 N, water-soluble CdSe nanocrystals, Rhodamine 5 N with Ag^{+}, Rhodamine 5 N before and after cation exchange. The concentration of Rhod-5 N, CdSe nanocrystals and Ag^{+} were 3 μM, 60 nM and 200 μM respectively

The level of the PRV antibody had a positive correlation with the concentration of the CdSe nanocrystals. To obtain a quantitative, sensitive and good linear relation in the immunoassay, the response of the Rhodamine 5 N to the CdSe nanocrystals should firstly be investigated. As shown in Fig. S1 in supporting information, the fluorescence intensity increased with the increment of the CdSe nanocrystals and reached the saturation fluorescence signals at 1,000 pM (the insert figure in Fig. S1). The linear part of this curve ranges from 1.0 to 500 pM. The detection limits, estimated as three times of the blank, were found to be 10 pM. The well response of the Rhodamine 5 N to CdSe indicated the method could be applied for detecting the PRV antibody sensitively.

Though all the reagents are analytical grade, other metal ions may also exist with very small amounts. Rhodamine 5 N also has been reported as a common calcium sensor and was suitable for measuring calcium ion from 10 μM to 1 mM [38].To confirm the good selectivity of the Rhodamine 5 N, the response of other common cations was examined. The signal caused by Cd^{2+} was 15 fold, 10 fold of Ca^{2+}, Zn^{2+} respectively. The signals of other cations were all very close to the background except the Pb^{2+} and Hg^{2+} had slightly higher background (Fig. S2 in supporting information). Considering

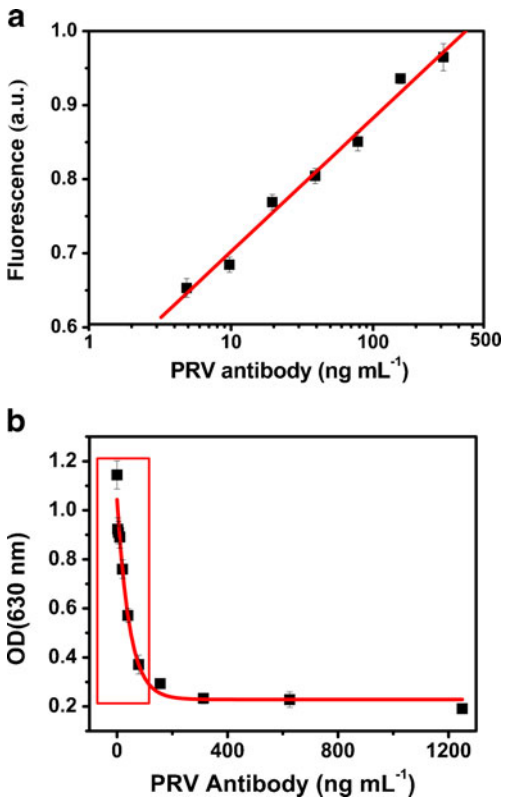

Fig. 4 (**A**) Detection of PRV antibody by CdSe nanocrystals based signal amplification method. (**B**) Calibration curve of conventional ELISA for PRV antibody. Each point depicted the average measurements of three times. Error bars represent the standard deviation of three times, the signals were all normalized

Table 1 Figures of merits of comparable methods for signal amplification in immunoassays

Method/Reagents(used)	Analyte	Analytical ranges	Detection limit	Ref.
Cation exchange/CdSe nanocrystals and Fluo-4	Human IgG	Not mentioned	0.05 $mgmL^{-1}$	[26]
Cation exchange/ZnSe nanocrystals and FluoZin3	Human IgE	1 $ngmL^{-1}$–100 $ngmL^{-1}$	1 $ngmL^{-1}$	[27]
Cation exchange/ZnS nanocrystals clusters and FluoZin3	Human IgE	5 $pgmL^{-1}$–100 $pgmL^{-1}$	5 $pgmL^{-1}$	[39]
Cation released by acid dissolution/ZnS nanocrysals and Fluozin-3	Mouse IgG	1 pM–0.5 nM	1 pM	[40]
Electrochemiluminescence/Quantum dots coated silica nanosphere	Rabbit IgG	5 $pgmL^{-1}$–10 $ngmL^{-1}$	1.3 $pgmL^{-1}$	[31]
Gold nanoparticle enhanced ELISA/gold Nanoparticle and antibody anti-CA15-3-HRP	CA15-3 antigen	Not mentioned	15 μgmL^{-1}	[17]
Cation exchange/CdSe Nanocrystals and rhodamine 5 N	PRV antibody	2.44 $ngmL^{-1}$–312 $ngmL^{-1}$	1.2 $ngmL^{-1}$	This work

the very rare existence of Pb^{2+} and Hg^{2+} in the material and reagents we used, the interference can be ignored.

Immune analyses of PRV antibody

Under the optimal condition, the performance of the method was evaluated by using the CdSe labeled secondary antibody to detect a serious PRV antibody with different concentration. As shown in Fig. 4A, the fluorescence intensity gradually increased with the increment of PRV antibody. A linear dependence between the fluorescence intensity and the PRV antibody levels was obtained in the range from 4.88 to 312 $ngmL^{-1}$ with a correlation coefficient of 0.9936. The linear equation was $Y=0.1803X+0.5220(R^2=0.9936)$ and the limit of detection (LOD) was as low as 1.22 ng (LOD, equal to 3× standard deviation above the blank). Now ELISA is the most common used method in PRV antibody detection, so we compared the results of the method with indirect ELISA. In ELISA, HRP labeled rabbit anti pig antibody was diluted 500 fold according to the suggestion of the manufactory. The results of ELISA were shown in Fig. 4B, with the increasing PRV antibody, the OD (630 nm) was decreased and there is a linear dependency from 4.18 to 78 $ngmL^{-1}$ as marked by the rectangle in Fig. 4B. The detection limits (calculated by the (background -signal) ≥0.4 and the signal/background ≤0.6) was 19.5 $ngmL^{-1}$. The linear equation was $Y=0.9285–0.0075X$ ($R^2=0.9548$). Compared with ELISA, the method owned a lower LOD and a wider linear range. The main reason maybe that: 1) signal detected in the ELISA was depended on the optical absorption which is less sensitive than the fluorescence detection in the method, 2) signal amplification by cation exchange further improved the

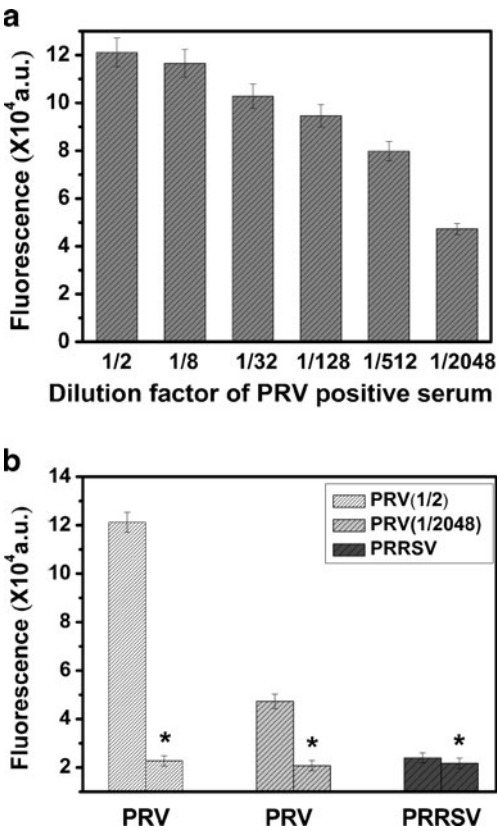

Fig. 5 (**A**) Histogram of the fluorescence intensity at different serum dilution ratios with the method. (**B**) The detection selectivity of the method for PRV antibody. *: The negative controls for each positive serum sample. Each point depicted the average measurements of three times. Error bars were calculated based on the standard deviation of three measurements

Table 2 Recovery test in the PRV negative and positive serum

Sample	Confirmed ($ng \cdot mL^{-1}$)	Added ($ng \cdot mL^{-1}$)	Detected ($ng \cdot mL^{-1}$)	Recovery ($ng \cdot mL^{-1}$)	RSD (%,n=5)
PRV negative serum					
1	0	9.76	8.91±0.48	91.3 %	4.9 %
2	0	19.52	21.53±0.82	110.3 %	4.2 %
3	0	39.04	38.84±0.62	99.4 %	1.6 %
4	0	71.08	63.05±0.84	88.7 %	1.2 %
PRV positive serum					
1	9.76	9.76	20.89±0.62	107.0 %	3.2 %
2	9.76	19.5	31.32±0.44	107.0 %	1.5 %
3	9.76	39.0	49.74±0.72	102.0 %	1.5 %
4	9.76	78.1	81.96±1.74	93.3 %	2.0 %

The results were based on mean value of five measurements

sensitivity. The lower detection limits and wider linear range in our method make it especially suitable for the early diagnose of the porcine pseudorabies. In the early porcine pseudorabies, the virus and antibody level is very low and the ELISA may not be able to detect it very effectively. The wider linear range also provides a more precise method for determining the antibody level in the serum which is very useful for evaluating the efficiency of vaccination and estimating the condition of the diseased swine. The CdSe labeled antibody is also cheaper, easily prepared and more stable than the enzyme labeled antibody. So, our method provides a novel and effective approach for the detection of porcine pseudorabies antibodies in clinical diagnosis.

A comparison of the merits of cation exchange method with those other methods based on signal amplification in immunoassays is shown in Table 1. As can be seen, compared with other signal amplification method, the cation exchange method can provide a very low detection limit to different analyte. Also, the cation exchange method is more simple and don't need some expensive and complex instruments, and a common luminescence spectrometer was adequate.

Detection of PRV antibody in clinical serum samples

The feasibility of the methods for the clinical samples was tested by analyzing a serious of positive serum samples (from piglet infected PRV) and negative serum (from piglet did not infect PRV). The serum was diluted to different concentrations by phosphate buffer with pH 7.4. The results of the immunoassay were shown in the Fig. 5A. With gradual dilution, the signal of the positive serum was decreased. Even with a 2,048 fold dilution, the signal was still almost 3 folds of the negative serum. The results suggested that the method had a good response to the PRV positive serum and can be used in clinic serum diagnose.

To verify the selectivity of the method, Porcine Reproductive and Respiratory syndrome virus (PRRSV) as a control group was investigated. A series of different level of positive serum of PRRSV was adopted as control group. As expected, the PRV serum yield gradually decreased signal with the decreasing of the concentration while the signals of PRRSV serum were almost invariant and close to the negative serum. The maximum and minimum (dilution factor were 4 and 2,048 respectively) signal of PRV, the average signal of PRRSV and negative samples were showed in Fig. 5B, even with a dilution factor of 2,048, the positive serum still owned a signal almost 3 folds of the PRRSV and negative serum. So it suggests that the developed methods both exhibit good selectivity.

The recovery test was performed using the PRV negative and positive serum by the standard addition method. Each recovery of PRV antibody was determined by comparing the results obtained before and after the addition of PRV antibody to the diluted serum samples. The results were listed in Table 2. The recoveries of serum samples with different level antibody were from 88.7 % to 110.3 % with a satisfying analytical precision (R.S.D$\leq$5.0 %), which validated the reliability and practicality of this method.

Conclusions

In conclusion, we have successfully developed a novel fluorescence signal amplification immunoassay for the PRV antibody. The method is based on the cation-exchange reaction in CdSe nanocrystals and the sensitive response of the Rhodamine 5 N to the Cd^{2+}. Compared with the traditional ELISA, the assay presented higher sensitivity, wider linear range and well specificity. The method was also very simple and low-cost. There are no strict requirements on optical, shapes or electrochemistry properties of the nanocrystals used in our method contrast with the common fluorescence, SERS and electrochemistry assay. The high sensitivity and selectivity of the serum samples assay demonstrated that the method was appropriate to use in the clinical diagnosis.

Acknowledgements The authors gratefully acknowledge the support for this research from National Natural Science Foundation of China (20975042, 21175051), the Fundamental Research Funds for the Central Universities (2010PY009, 2011PY139) and the Natural Science Foundation of Hubei Province Innovation Team (2011CDA115).

References

1. Baskerville A, McFerran J, Dow C (1973) Aujeszky's disease in pigs. Vet Bull 43:456480
2. Zanin E, Capua I, Casaccia C, Zuin A, Moresco A (1997) Isolation and characterization of Aujeszky's disease virus in captive brown bears from Italy. J Wildl Dis 33:632634
3. Iglesias G, Pijoan C, Molitor T (1992) Effects of pseudorabies virus infection upon cytotoxicity and antiviral activities of porcine alveolar macrophages. Comp Immunol Microbiol Infect Dis 15:249259
4. Iglesias G, Pijoan C, Molitor T (1989) Interactions of pseudorabies virus with swine alveolar macrophages: Effects of virus infection on cell functions. J Leukoc Biol 45:410415
5. Bolin S, Bolin C (1984) Pseudorabies virus infection of six-and ten-day-old porcine embryos. Theriogenology 22:101108
6. Muller T, Hahn E, Tottewitz F, Kramer M, Klupp B, Mettenleiter T, Freuling C (2011) Pseudorabies virus in wild swine: a global perspective. Arch Virol 156:115
7. Ruiz-Fons F, Segales J, Gortazar C (2008) A review of viral diseases of the European wild boar: effects of population dynamics and reservoir role. Vet J 176:158169
8. Boadella M, Gortazar C, Vicente J, Ruiz-Fons F (2012) Wild boar: an increasing concern for Aujeszky's disease control in pigs? BMC Vet Res 8:7
9. Ostrowski M, Galeota J, Jar A, Platt K, Osorio FA, Lopez O (2002) Identification of neutralizing and nonneutralizing epitopes in the porcine reproductive and respiratory syndrome virus GP5 ectodomain. J Virol 76:42414250
10. He Q, Velumani S, Du Q, Lim CW, Ng FK, Donis R, Kwang J (2007) Detection of H5 avian influenza viruses by antigen-capture

enzyme-linked immunosorbent assay using H5-specific monoclonal antibody. Clin Vaccine Immunol 14:617623
11. Xu XG, Chen GD, Huang Y, Ding L, Li ZC, Chang CD, Wang CY, Tong DW, Liu HJ (2012) Development of multiplex PCR for simultaneous detection of six swine DNA and RNA viruses. J Virol Methods 183:6974
12. Yue F, Cui S, Zhang C, Yoon KJ (2009) A multiplex PCR for rapid and simultaneous detection of porcine circovirus type 2, porcine parvovirus, porcine pseudorabies virus, and porcine reproductive and respiratory syndrome virus in clinical specimens. Virus genes 38:392397
13. Dong H, Li CM, Chen W, Zhou Q, Zeng ZX, Luong JHT (2006) Sensitive amperometric immunosensing using polypyrrolepropylic acid films for biomolecule immobilization. Anal Chem 78:74247431
14. Wilson MS, Nie W (2006) Electrochemical multianalyte immunoassays using an array-based sensor. Anal Chem 78:25072513
15. Yin Z, Liu Y, Jiang LP, Zhu JJ (2011) Electrochemical immunosensor of tumor necrosis factor α based on alkaline phosphatase functionalized nanospheres. Biosens Bioelectron 26:18901894
16. Zhao H, Sheng Q, Zheng J (2012) Direct electrochemistry and electrocatalysis of horseradish peroxidase on a gold electrode modified with a polystyrene and multiwalled carbon nanotube composite film. Microchim Acta 176:18
17. Ambrosi A, AiroF MA (2009) Ehanced gold nanoparticle based ELISA for a breast cancer biomaker. Anal Chem 82:11511156
18. Manclús JJ, Abad A, Lebedev MY, Mojarrad F, Micková B, Mercader JV, Primo J, Miranda MA, Montoya A (2004) Development of a monoclonal immunoassay selective for chlorinated cyclodiene insecticides. J Agric Food Chem 52:27762784
19. Kuhlmann W, Peschke P (1986) Glucose oxidase as label in histological immunoassays with enzyme-amplification in a two-step technique: coimmobilized horseradish peroxidase as secondary system enzyme for chromogen oxidation. Histochem Cell Biol 85:1317
20. Suzuki A, Itoh F, Hinoda Y, Imai K (1995) Double determinant immunopolymerase chain reaction: a sensitive method for detecting circulating antigens in human sera. Cancer Sci 86:885889
21. Yazynina EV, Zherdev AV, Dzantiev BB, Izumrudov VA, Gee SJ, Hammock BD (1999) Immunoassay techniques for detection of the herbicide simazine based on use of oppositely charged water-soluble polyelectrolytes. Anal Chem 71:35383543
22. Chen Y, Ren H, Liu N, Sai N, Liu X, Liu Z, Gao Z, Ning B (2010) A fluoroimmunoassay based on quantum dot-streptavidin conjugate for the detection of chlorpyrifos. J Agric Food Chem 58:88958903
23. Luo Z, Chen K, Lu D, Han H, Zou M (2011) Synthesis of p-aminothiophenol-embedded gold/silver core-shell nanostructures as novel SERS tags for biosensing applications. Microchim Acta 173:149156
24. Ma C, Xie G, Zhang W, Liang M, Liu B, Xiang H (2012) Label-free sandwich type of immunosensor for hepatitis C virus core antigen based on the use of gold nanoparticles on a nanostructured metal oxide surface. Microchim Acta 178:110
25. Tian J, Huang J, Zhao Y, Zhao S (2012) Electrochemical immunosensor for prostate-specific antigen using a glassy carbon electrode modified with a nanocomposite containing gold nanoparticles supported with starch-functionalized multi-walled carbon nanotubes. Microchim Acta 178:18
26. Li J, Zhang T, Ge J, Yin Y, Zhong W (2009) Fluorescence signal amplification by cation exchange in ionic nanocrystals. Angew Chem Int Ed 48:15881591
27. Yao J, Schachermeyer S, Yin Y, Zhong W (2011) Cation exchange in ZnSe nanocrystals for signal amplification in bioassays. Anal Chem 83:402408
28. Sheng Z, Hu D, Zhang P, Gong P, Gao D, Liu S, Cai L (2012) Cation exchange in aptamer conjugated CdSe nanoclusters: a novel fluorescence signal amplification for cancer cell detection. Chem Commun 48:42024204
29. Hu D, Han H, Zhou R, Dong F, Bei W, Jia F, Chen H (2008) Gold (III) enhanced chemiluminescence immunoassay for detection of antibody against ApxIV of Actinobacillus pleuropneumoniae. Analyst 133:768773
30. Sheng Z, Han H, Hu D, Liang J, He Q, Jin M, Zhou R, Chen H (2009) Quantum dots-gold (III)-based indirect fluorescence immunoassay for high-throughput screening of APP. Chem Commun 45:25592561
31. Qian J, Zhang C, Cao X, Liu S (2010) Versatile immunosensor using a quantum dot coated silica nanosphere as a label for signal amplification. Anal Chem 82:64226429
32. Qu L, Peng X (2002) Control of photoluminescence properties of CdSe nanocrystals in growth. J Am Chem Soc 124:20492055
33. Gao J, Chen K, Xie R, Xie J, Lee S, Cheng Z, Peng X, Chen X (2010) Ultrasmall near-infrared non-cadmium quantum dots for in vivo tumor imaging. Small 6:256261
34. Breus VV, Heyes CD, Nienhaus GU (2007) Quenching of CdSe-ZnS core-shell quantum dot luminescence by water-soluble thiolated ligands. J Phys Chem C 111:1858918594
35. Ipe BI, Shukla A, Lu H, Zou B, Rehage H, Niemeyer CM (2006) Dynamic light scattering analysis of the electrostatic interaction of hexahistidine tagged cytochrome P450 enzyme with semiconductor quantum dots. Chem Phys Chem 7:11121118
36. Soibinet M, Souchon V, Leray I, Valeur B (2008) Rhod-5 N as a fluorescent molecular sensor of cadmium (II) ion. J Fluoresc 18:10771082
37. Son DH, Hughes SM, Yin Y, Alivisatos AP (2004) Cation exchange reactions in ionic nanocrystals. Science 306:10091012
38. Ribou AC, Salmon JM, Vigo J, Goyet C (2007) Measurements of calcium with a fluorescent probe Rhod-5 N: Influence of high ionic strength and pH. Talanta 71:437442
39. Yao J, Han X, Zeng S, Zhong W (2012) Detection of femtomolar proteins by nonfluorescent ZnS nanocrystal clusters. Anal Chem 84:1645–1652
40. Cowles CL, Zhu X, Publicover NG (2011) Fluorescence signal transduction mechanism for immunoassay based on zinc ion release from ZnS nanocrystals. Analyst 136:2975–2980